Kinetics of He–Hg, Ne–Tl, and Ne–Ga active media in pulsed ion HCD metal vapor lasers

I.G. Ivanov and M.F. Sem

Rostov State University

Received October 7, 2001

The dependences of ion laser level density, gain, and output power on the parameters of hollow cathode discharge (HCD) for Hg^+, Tl^+ and Ga^+ lasing transitions pumped due to inelastic thermal charge-transfer collisions with simultaneous excitation are studied both theoretically and experimentally. The transitions involved in these processes are 7p ^{2}P–7s ^{2}S and 7p ^{2}P–6d ^{2}D Hg II in He–Hg mixture and np^{1,3}P–ns ^{1,3}S and np ^{1,3}P–(n–1)d ^{1,3}D Tl II (n=7) and Ga II (n=5) in the Ne–Tl mixture and Ne–Ga mixture, respectively (these mixtures are most efficient laser media for pulsed HCD lasers). A detailed kinetic model is developed based on statement that the total charge transfer rate for all pumped metal levels is equal to buffer gas ionization rate because in HCD negative glow (NG) the decay rate of the buffer gas ion by charge-transfer process is higher than that due to ambipolar diffusion. This model allows for the collisions of excited metal ions with thermal electrons and atoms that lead to ion excitation or de-excitation and uses the transition probabilities calculated in the Coulomb approximation with the account for resonance trapping. It also uses the partial charge-transfer cross sections calculated based on Landau–Zener theory and the Wigner's spin rule and corrected against the experimental data. The NG thermal electron temperature and other discharge parameters typical of HCD are calculated. The results calculated for the known laser transitions are in a good agreement with the experimental data and are used for prediction of laser parameters on new IR transitions.

Introduction

The advantages of negative glow (NG) of hollow cathode discharge (HCD) for excitation of the lasing transitions by inelastic collisions in plasma over positive column discharge are generally known. For the first time, the HCD was used in atomic neon laser, however, then it was found that HCD is more efficient for ion transitions in metals and heavy inert gases. The number of such lasing media now reached 26, and the number of ion lasing transitions in them equals 280 (Refs. 1 and 2).

Since the HCD lasers tend to generation of a spatially inhomogeneous discharge, the optimum pump power has been obtained for only few transitions in the stationary mode of operation, whereas the output power at the rest lines does not reach maximum values. At the same time, if short (0.1–10 μs) pulses are used to excite the discharge, the discharge inhomogeneities have no time to develop and the optimum pump level can be applied to the medium. In this case, the mean deposited power and the output power can be controlled by varying the pulse repetition frequency.

Regardless the facts that the first HCD lasers were excited by microsecond pulses,[1] the power and plasma characteristics of even most efficient pulsed HCD lasers (mercury,[1,3] thallium,[3–6] gallium,[7] krypton,[8] cadmium, and zinc[1] lasers, as well as lasers using mixtures of these elements as an active medium) are not still thoroughly studied.

Lasing at three mercury ion doublet transitions $7p\ ^2P_{3/2,1/2}$–$7s\ ^2S_{1/2}$ and $7p\ ^2P_{3/2}$–$6d\ ^2D_{5/2}$ was observed in a mixture with helium in both pulsed and stationary HCD, and the orange line with the wavelength of 615 nm ($7p\ ^2P_{3/2}$–$7s\ ^2S_{1/2}$ transition) had the best characteristics: the pulse power and the mean output power were, respectively, 22 and 0.88 W at the current pulse duration of about 1 μs, the pulse repetition frequency of 40 kHz, the cathode diameter of 2 cm, and the length of 40 cm (Ref. 3). (The term diagram of the mercury ion can be found in most of the reference books.) The energy of excitation of the upper 7^2P levels is close to the energy of ionization of helium (24.56 eV), and the mechanism of pumping the lasing $7p\ ^2P$–$7s\ ^2S$ and $7p\ ^2P$–$6s\ ^2D$ transitions in the He–Hg mixture is an exothermal reaction of charge-transfer collisions of the buffer inert gas (helium) ions with metal (mercury) atoms with the subsequent ionization and excitation of the latter. This reaction occurs in the gas-discharge plasma at particle thermal rates[1–3]:

$$R_0^+ + M_0 \Rightarrow R_0 + M^{+*}(7p\ P_J) + \Delta E(\infty), \qquad (1)$$

where R_0 and R_0^+ denote helium atoms in the ground and ionized states, and M_0 and M^{+*} denote mercury atoms in the ground state and excited mercury ions; $\Delta E(\infty)$ is the energy difference between R_0^+ and M^{+*} at a sufficiently large separation between the particles. The total effective charge-transfer cross section in the He^+–Hg mixture exceeds the gas-kinetic one: $Q^{\text{total}} = 1.4 \cdot 10^{-14}\ \text{cm}^{-2}$ (Ref. 1).

Lasing at thallium ion transitions was observed at F–D Tl II transitions in a mixture of thallium vapor

0235-6880/01/11 934-06 $02.00

with helium and, with a far higher efficiency, on the P–S Tl II transitions in a mixture with neon.[1,4,5] The most attractive, from the viewpoint of possible applications, is lasing at the yellow Tl II line with $\lambda = 594.95$ nm ($7p^3\ P_2^\circ - 7s^3S_1$ transition). At this line, the pulse power and the mean output power in the repetitively pulsed mode in HCD (27 W and 285 mW, respectively[3]), like in mercury, exceed by several orders of magnitude the power in the continuous-wave (cw)[4] and quasi-cw[6] modes.

The diagram of the Tl II lower singlet and triplet terms is depicted in Fig. 1. The mechanism of pumping of all known laser singlet and triplet $7p\ ^{1,3}P$–$7s\ ^{1,3}S$ transitions in the Ne–Tl mixture is the charge transfer collisions of the buffer inert gas (neon) atoms with thallium atoms.[4] The total effective charge-transfer cross section in the Ne–Tl mixture is $Q^{\text{total}} = 3 \cdot 10^{-15}$ cm^{-2} (Ref. 4).

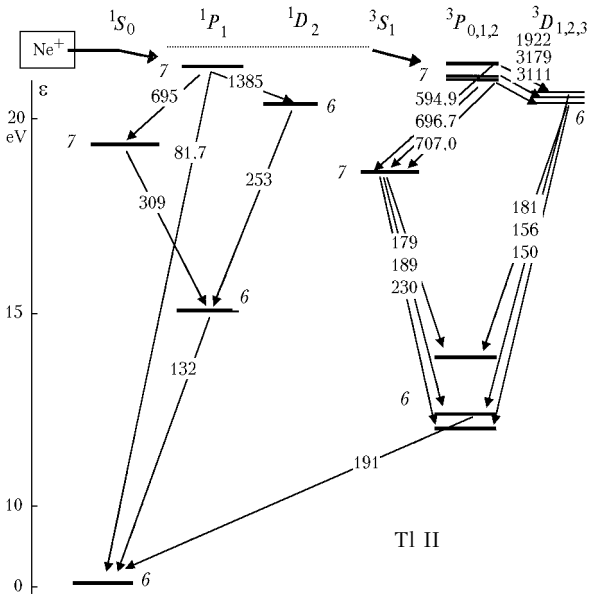

Fig. 1. Diagram of the lower energy levels of thallium ions (transition wavelengths, in nm, are given nearby the arrows).

The ion spectrum of gallium is similar to that of thallium, the known lasing $5p^{1,3}P$–$4s^{1,3}S$ transitions in gallium ion are also populated due to charge transfer process in Ne–Ga mixture, and the gain achievable in HCD is of the same order of magnitude as in thallium.[7]

Below we consider the kinetics of formation of the population inversion at known ion lasing $7p^2P$–$7s^2S$ and $7p\ ^2P$–$6d\ ^2D$ Hg II transitions pumped in the HCD plasma due to charge transfer at collisions of helium ions with the mercury atoms, as well as at $np\ ^{1,3}P$–$ns^{1,3}S$ thallium ($n = 7$) and gallium ($n = 5$) transitions pumped due to charge transfer at collisions of neon ions with metal atoms. The inversion and the gain at $np\ ^{1,3}P - (n-1)d\ ^{1,3}D$ Tl II and Ga II IR transitions potentially suitable for using as an active medium in Ne–Tl and Ne–Ga HCD lasers are calculated as well.

Computational technique

The HCD plasma is generated at a sufficiently low pressure of the main (buffer) gas usually not exceeding 20–30 Torr. This fact significantly simplifies the analysis. A feature of the HCD NG is sufficiently high optimal pressure and the concentration of ionizable metal atoms (0.1–0.3 Torr and ~$2 \cdot 10^{15}$–10^{16} cm^{-3}), roughly, two orders of magnitude exceeding the concentration of the metal in the positive column. Nevertheless, the number of fast primary electrons in the HDC NG is larger than in the Maxwell distribution. This is explained by the unique process of electron acceleration in the cathode dark space and determines high efficiency of ionization of the buffer inert gas (in the helium or neon mixtures considered here) and high efficiency of further energy transfer to metal ions in the charge transfer process. The number of slow "secondary" (thermal) electrons n_e^{thermal} with the nearly Maxwell distribution and the temperature $T_e \sim 0.1 \ldots 1$ eV that arise at ionization is also increased.

As we have shown earlier,[1–3] the pulsed mode of HCD is characterized by higher density and energy of fast electrons, whose number achieves limiting values already in 0.5 to 1 μs after the beginning of the current pulse, with the number of slow electrons monotonically increasing in time. We can believe that the number of electrons in both of these groups varies proportionally at the constant duration of a current pulse with the varying amplitude. Thermal electrons give rise to electronic excitation and de-excitation of energetically close levels. For most of the transitions pumped by charge transfer, this leads to saturation and breakdown of inversion at some, specific for every transition, critical concentration $(n_e^{\text{thermal}})^{\text{crit}}$. Earlier we have found this effect for the He–Hg mixture.[9]

For the Doppler profile of the lasing transition of an ion metal-vapor laser between the upper (i) and lower (k) levels, whose population density is, respectively, N_i and N_k, the unsaturated gain is

$$\alpha_{ik} = 1.7 \cdot 10^{-27}\ (\mu/T)^{1/2}\ A_{ik}\ \lambda_{ik}^3 \times \times g_i\ \{N_i/g_i - N_k/g_k\}\ \chi_{ik}, \qquad (2)$$

where λ_{ik} is the wavelength, in nm; μ and T are the mass of the ion M^{+*} and the gas temperature, in K; χ_{ik} is the factor of isotopic and (or) superfine splitting of a line, $\chi \le 1$ (isotopic splitting takes place for the Hg II transition with $\lambda = 615$ nm, and superfine splitting prevails over the isotopic one for Tl II and Ga II ion transitions[10]); g is the statistical weight of a level, $g = 2J + 1$; A_{ik} is the Einstein coefficient.

The populations N_i for the S, P, and D levels of mercury, thallium, and gallium ions that are needed in calculating the gain at $np\,P$–$ns\,S$ and $np\,P - (n-1)d\,D$ transitions of Hg II, Tl II ($n = 7$), and Ga II ($n = 5$) (see the diagram for Tl II in Fig. 1) were calculated by solving the system of kinetic equations allowing for all

transitions between the levels possible in low-pressure plasma:

$$dN_i/dt = \xi_i (W_{ch\text{-}t})^{total} + \sum_{j>i} A_{ji} N_j +$$

$$+ \sum_{m\neq i} \{<q_{mi} \nu_e> n_e^{thermal} + <Q_{mi}\ ^R V^R> N_0^R +$$

$$+ <Q_{mi}\ ^M V^M> N_0^M\} N_m - \sum_{k<i} \{A_{ik} + \hat{g}_{i0} A_{i0}\} N_i -$$

$$- \sum_{m\neq i} \{<q_{im} \nu_e> n_e^{thermal} + <Q_{im}\ ^R V^R> N_0^R +$$

$$+ <Q_{im}\ ^M V^M> N_0^M\} N_i = 0, \quad (3)$$

where $W_i = \xi_i (W_{ch\text{-}t})^{total}$ is the rate of pumping this level directly by charge transfer; ξ_i is the coefficient of partial charge transfer to the given level; ($\xi_i \le 1$, and $\sum \xi_i = 1$); $\hat{g}_{i0} A_{i0}$ is the probability of the resonance transition of the M_0^+ ion into the ground state with the allowance for radiation trapping; $\hat{g}_{i0}$ is the Iberian–Holstein factor,[11] $<q_{mi} \nu_e>$ and $<q_{im} \nu_e>$ are the constants of excitation and de-excitation of the $i$tch level at collisions with thermal electrons[1]; $<Q_{mi}\ ^R V^R>$, $<Q_{mi}\ ^M V^M>$ and $<Q_{im}\ ^R V^R>$, $<Q_{im}\ ^M V^M>$ are the same at collisions with the neon (R) and metal (M) atoms:

$$<q_{mi} \nu_e> = 3.2 \cdot 10^{-6} f_{mi} T_e^{-1/2} \Delta\varepsilon_{im}^{-1} g_m/g_i;$$

$$<q_{im} \nu_e> = 3.2 \cdot 10^{-6} f_{mi} T_e^{-1/2} \Delta\varepsilon_{im}^{-1} \exp(-T_e^{-1} \Delta\varepsilon_{imp}),$$

$$<Q_{mi}\ ^R V^R> = <Q_{im}\ ^R V^R> \exp(-T_g^{-1} \Delta\varepsilon_{imp}),$$

$$<Q_{mi}\ ^M V^M> = <Q_{im}\ ^M V^M> \exp(-T_g^{-1} \Delta\varepsilon_{im}),$$

f_{mi} is the oscillator strength of a transition; T_e is the temperature of thermal (slow) electrons, in eV; T_g is the gas temperature, in eV; $\Delta\varepsilon_{im}$ is the energy difference between levels, in eV; V^R and V^M are the relative speeds of buffer gas–metal and metal–metal atoms, respectively. The Einstein coefficients A_{ji} were calculated in the Coulomb approximation, which is well satisfied for Hg II, Tl II, and Ga II.

For the ith upper metal lasing level, taking into account that the buffer gas ions (R_0^+) leave this elementary volume at low pressure only due to diffusion, recombination, and charge transfer, we obtain

$$W_i = \frac{W(R^+)\ N(M_0)\ \xi_i\ K_{ch\text{-}t}}{\nu(R^+) + N(M_0)\ K_{ch\text{-}t}}, \quad (4)$$

where $W(R^+)$ is the gas ionization rate; $N(M_0)$ is the concentration of metal atoms in the ground state; $K_{ch\text{-}t} = <QV_{rel}>$ is the charge-transfer reaction constant, Q is the total charge-transfer cross section; V_{rel} is the relative speed of the R^+ and M_0 atoms before the interaction; $\xi_i Q$ is the cross section of partial charge transfer to the ith level, $\nu(R^+)$ is the total rate of deactivation (departure) of the buffer gas ions R^+ from the volume (through ambipolar diffusion and recombination).

At the concentration of metal atoms in the HCD NG plasma $N(M_0) \ge \nu(R^+)/K_{ch\text{-}t} \sim 10^{15}$ cm^{-3} (what is optimal for ion HCD lasers), destruction of ions of the buffer gas R_0^+ through the charge transfer turns out to be the main mechanism of their deactivation (the first term in the denominator of Eq. (4) is far smaller than the second), and then[9,12]

$$W_i \cong \xi_i\ W(R^+). \quad (5)$$

The total rate of charge-transfer pumping of all metal levels $(W_{ch\text{-}t})^{total}$ is equal to the rate of ionization of the buffer gas:

$$(W_{ch\text{-}t})^{total} = \sum_i \xi_i\ W(R^+) = W(R^+) \quad (6)$$

and independent of the charge-transfer cross section.

Believing that the function of ionization of the buffer gas $q_i(\varepsilon)$, as well as the electron energy distribution function, above the gas ionization threshold is a slowly varying function of the energy of fast electrons ε and neglecting the contribution of electrons with the energy near the ionization threshold ε_{thr} to ionization, we obtain for $W(R^+)$ the following expression:

$$W(R^+) = N(R_0) \int_{\varepsilon=\varepsilon_{thr}}^{\infty} f(\varepsilon)\ q_i(\varepsilon)\ \varepsilon\ d\varepsilon \approx$$

$$\approx A n_e^{fast} \approx B n_e^{thermal}. \quad (7)$$

On the other hand, since slow secondary electrons are generated at every buffer gas ionization event, we can obtain from the continuity equation that

$$W(R^+) = (\nu_e^{dif} + \nu_e^{recomb})\ n_e^{thermal}, \quad (8)$$

i.e., the constant B in Eq. (7) has the meaning of the sum frequency of diffusion and recombination departure of electrons from this volume element. In this case, if $\nu_e^{dif} \gg \nu_e^{recomb}$, then $B \approx \nu_e^{dif}$.

Results and discussion

Despite the fact that the charge-transfer reaction in the helium–mercury vapor mixture is being investigated for a long time, because the He–Hg laser was the first ion metal-vapor laser, the results of determination of the cross sections of partial charge transfer to the 7^2P, 7^2S, and 6^2D levels of Hg II are rather contradictory (see Table 1a). Actually, the measured rates of pumping the lasing transitions in a stationary discharge[14] (when the processes of level mixing by collisions with electrons are weak) and by the methods of modulation in a pulsed discharge[16] confirm the first calculated data[13] that the level $7p^2P_{3/2}$, for which the energy defect $\Delta E(\infty)$ is the lowest one is, roughly, populated by an order of magnitude denser than the level $7p^2P_{1/2}$, as well as

than the levels $7s^2S$ and $6d^2D$. At the same time, according to data from Refs. 15 and 17, the cross sections of partial charge transfer to the levels $7p^2P_{3/2}$ and $7p^2P_{1/2}$ are close, and according to Ref. 18 the ratio of these cross sections (and the coefficients ξ_i) turns out to be reverse for them. In this connection, we calculated the coefficients of the partial charge-transfer ξ_i by the Landau–Zener theory[13,19] for all levels of the mercury ion with $0 < \Delta E(\infty) < 1.5$ eV, including the Beitler levels, so that $\Sigma\xi_i = 1$. The values of these coefficients are given in Table 1a. The levels $^4D_{1/2}$ and $^4D_{7/2}$, for which the Wigner's spin rule does not usually work, were excluded from the consideration.

Table 1a. Coefficients of the partial charge transfer at collisions with He^+ to different ion levels of Hg II ($\xi_i = Q_i^{partial}/Q^{total}$)

Parameter	Levels			
	$7p\ ^2P_{3/2}$	$7p\ ^2P_{1/2}$	$6d\ ^2D_{5/2}$	$6d\ ^2D_{3/2}$
$\Delta E(\infty)$, eV	0.27	0.72	1.06	1.18
ξ_i:				
This work	0.22	0.023	0.038	0.025
Ref. 13, rel. units	78	12	5.8	4.2
Ref. 14	0.22	0.03		
Ref. 15	0.65	0.35		
Ref. 16, rel. units	20	3.6	2.4	
Ref. 17, rel. units	7	8		
Ref. 18, rel. units	4.97	80.2	0.548	1.89

The data on the cross sections of partial charge transfer at collisions with neon to the levels $np\ ^{1,3}P$ and $(n-1)d\ ^{1,3}D$ of the thallium ($n = 7$) and gallium ($n = 5$) ion are absent in the literature. Therefore, we calculated them as well based on the Landau–Zener theory for all Tl II and Ga II levels with $0 < \Delta E(\infty) < 1.5$ eV with the allowance for the Wigner's spin rule (see Tables 1b and c).

Table 1b. Coefficients of partial charge transfer at collisions with Ne^+ to different ion levels of Tl II ($\xi_i = Q_i^{partial}/Q^{total}$)

Parameter	Levels						
	$7p\ ^3P_2$	$7p\ ^3P_1$	$7p\ ^3P_0$	$7p\ ^1P_1$	$6d\ ^3D_3$	$6d\ ^3D_2$	$6d\ ^3D_1$
$\Delta E(\infty)$, in eV	0.33	0.64	0.66	0.28	0.976	1.02	1.06
ξ_i	0.40	0.073	0.023	0.28	0.11	0.074	0.04

Table 1c. Coefficients of partial charge transfer at collisions with Ne^+ to different ion levels of Ga II ($\xi_i = Q_i^{partial}/Q^{total}$)

Parameter	Levels			
	$5p\ ^3P_2$	$5p\ ^3P_1$	$5p\ ^3P_0$	$5p\ ^1P_1$
$\Delta E(\infty)$, in eV	0.84	0.87	0.88	0.62
ξ_i	0.37	0.22	0.08	0.33

It can be seen that for Tl II the coefficient of partial charge transfer is maximum ($\xi_i = 0.4$) for the level 7^3P_2 due to the lowest energy defect $\Delta E(\infty)$ for this level and its highest statistical weight g_i. For the $5p\ ^1P_1$ and $5p\ ^3P_{2,1,0}$ levels of Ga II, the values of $\Delta E_i(\infty)$ are close and the partial coefficients ξ_i are roughly proportional to their statistical weights g_i.

Atom-atom collisions play a significant role for transitions between the multiplet levels $7p\ ^2P$ of Hg II, $7p\ ^{1,3}P$ of Tl II, and $5p\ ^{1,3}P$ of Ga II. Their cross sections entering into $\langle Q_{mi}\ ^{R}V^{R}\rangle$, $\langle Q_{mi}\ ^{M}V^{M}\rangle$ and $\langle Q_{im}\ ^{R}V^{R}\rangle$, $\langle Q_{im}\ ^{M}V^{M}\rangle$ were calculated using data from Ref. 20 and had the values of about 10^{-16}–10^{-15} cm^2 for the Hg^+–Hg, Tl^+–Tl, and Ga^+–Ga collisions and 10^{-18} cm^2 for the Hg^+–He, Tl^+–Ne, and Ga^+–Ne (Ref. 21) collisions. The frequencies of the direct and inverse transitions were related using the principle of detailed balance.[11]

The values of the reduced level density $N_i(M^{+*})/g_iW(R^+)$ (where $g_i = 2J_i + 1$ is the statistical weight of the level) as functions of $n_e^{thermal}$ found for each mixture from solution of the systems of kinetic equations are specific for every type of levels.

Figure 2 depicts the reduced population for the singlet (Fig. 2*a*) and triplet (Fig. 2*b*) levels of Tl II. It can be seen that for small $n_e^{thermal}$ the reduced level density is constant, and the dependence of N_i on $W(R^+)$ is close to a linear one. As $n_e^{thermal}$ increases (with the increasing current density), the level density is redistributed mostly due to de-excitation collisions with the electrons and atoms. As a results, the upper levels (P and S) are additionally de-populated (the reduced level density tends to decrease), whereas the lower levels $\{(n-1)D$ and $(n-1)P\}$ are additionally populated (the reduced level density begins to grow, achieves the maximum, and then decreases).

At the same time, for the resonance doublet $7p\ ^2P_{3/2,1/2}$ levels of Hg II and the resonance singlet $7p\ ^1P_1$ levels of Tl II and $5p\ ^1P_1$ levels of Ga II, their lifetime increases monotonically with the increase of the electron density because $n_e \approx N(M_0^+)$ (Ref. 9) and due to trapping of the resonance radiation. At the intermediate values of $n_e^{thermal}$ (10^{13} cm^{-3} for Tl II in Fig. 2*a*), this even increases somewhat the reduced level density.

The point of intersection of the curves for the pairs of the levels P–S and P–D connected by an optical transition corresponds to disappearance of the population inversion and gives the value of $n_e^{critical}$ (i.e., inversion occurs at $n_e \le n_e^{critical}$). The value of $n_e^{critical}$ decreases with decreasing T_e. Thus, for the Tl II transition $7p\ ^3P_2^\circ$–$7s\ ^3S_1$ ($\lambda = 594.95$ nm) at $T_e = 0.5$ and 1.0 eV, the critical density $n_e^{critical}$ equals $2 \cdot 10^{14}$ and $3.5 \cdot 10^{14}$ cm^{-3}, respectively.

The dependence of $N_i/g_iW(R^+)$ on $n_e^{thermal}$ for the four transitions in Hg II, nine transitions in Tl II, and eight transitions in Ga II was used in calculating the dependence $\alpha_{ik}/W(R^+) = \varphi(n_e^{thermal})$, as well as the dependence $\alpha_{ik}(n_e^{thermal}) \equiv \alpha_{ik}(J_{disch})$, by Eq. (7).

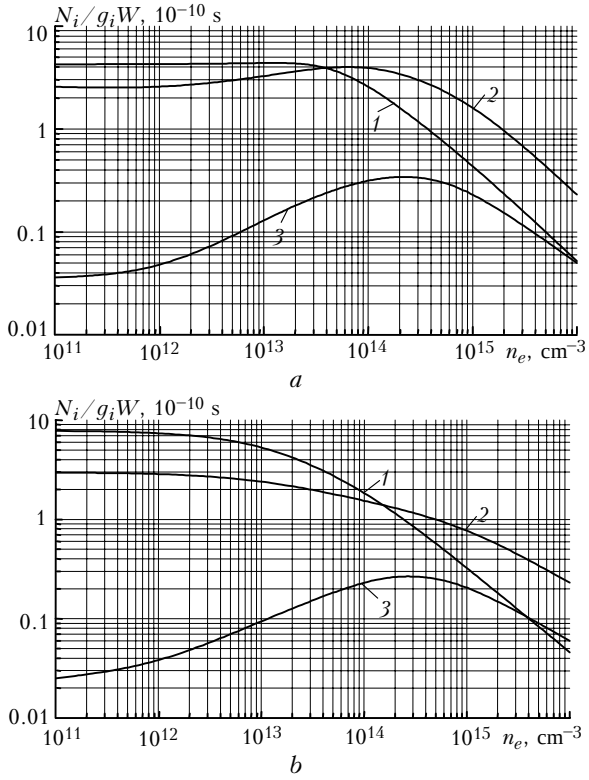

Fig. 2. Dependence of N_i/g_iW on the electron concentration n_e for singlet (*a*) and triplet (*b*) levels of Tl II; Fig. 2*a*: the level $7p^1P_1$ (curve *1*), $7s^1S_0$ (*2*), $6d^1D_2$ (*3*); $T_e = 0.5$ eV; Fig. 2*b*: level $7p^3P_2$ (*1*), $7s^3S_1$ (*2*), and $6d^3D_3$ (*3*).

Table 2a gives the values of the gain $\alpha_{ik}^{\max}$, as well as the corresponding values of $(n_e^{\text{thermal}})^{\text{opt}}$ and J_{opt} for these transitions at a fixed, typical of HCD, value of the electron temperature $T_e = 0.5$ eV. This corresponds to the fixed duration (about 0.5 μs) of the discharge current pulse. It also gives the line splitting factors χ_{ik} calculated for all transitions according to Ref. 10 and checked by us earlier for the *P*–*S* transitions of Tl II (Ref. 5). Since Eq. (2) includes the factor χ_{ik}, the obtained value of $\alpha_{ik}^{\max}$ can be compared with the available experimental data. Therefore, Tables 2a–c also give the experimental values of the gain for transitions in the visible range measured in Refs. 1, 3, 5, and 7. It can be seen that the ratio of theoretical α_{ik} calculated in relative units and the ratio of experimental α_{ik}^{exp} for the well known most intense lasing lines agree rather well.

Table 2a. Calculated and measured gain α_{ik} for transitions of Hg II ($T_e = 0.5$ eV)

Transition	λ, nm	$n_e^{\text{opt}} \times 10^{13}$, cm^{-3}	J_{opt}, A/cm^2	χ	α, rel. units	α^{exp}, 10^{-2}, cm^{-1} Refs.1 and 3
$7p^2P_{3/2}$–$7s^2S_{1/2}$	614.9	13	0.9	0.3	0.012	7.0
$7p^2P_{1/2}$–$7s^2S_{1/2}$	794.5	7.9	0.54	1	0.0125	8.0
$7p^2P_{3/2}$–$6d^2D_{5/2}$	1555	260	18	0.3	1	
$7p^2P_{1/2}$–$6d^2D_{3/2}$	3016	440	30	1	0.75	

Table 2b. Calculated and measured gain α_{ik} for transitions of Tl II ($T_e = 0.5$ eV)

Transition	λ, nm	$n_e^{\text{opt}} \times 10^{13}$, cm^{-3}	J_{opt}, A/cm^2	χ	α, rel. units.	α^{exp}, 10^{-2}, cm^{-1} Refs. 3 and 5
$7p^3P_2$–$7s^3S_1$	594.9	4	0.9	0.42	0.16	3.5
$7p^3P_1$–$7s^3S_1$	696.7	0.2	0.022	0.39	0.00046	–
$7p^3P_0$–$7s^3S_1$	707.0	1.1	0.17	0.47	0.0041	0.9
$7p^1P_1$–$7s^1S_0$	695.0	1.5	0.17	0.47	0.074	2.0
$7p^1P_1$–$7s^3S_1$	582.9	5	0.55	0.39	0.0018	0.3
$7p^3P_2$–$6d^3D_3$	1922	30	2.4	0.57	1	
$7p^3P_1$–$6d^3D_2$	3179	80	6.9	0.6	0.23	
$7p^3P_0$–$6d^3D_1$	3111	200	27.7	0.67	0.13	
$7p^1P_1$–$6d^1D_2$	1385	200	20.7	0.6	0.85	

Table 2c. Calculated and measured gain α_{ik} for transitions of Ga II ($T_e = 0.5$ eV)

Transition	λ, nm	$N_e^{\text{opt}} \times 10^{13}$, cm^{-3}	J_{opt}, A/cm^2	χ	α, rel. units	α^{exp}, 10^{-2}, cm^{-1} Ref. 7
$5p^3P_2$–$5s^3S_1$	633.42	2	0.34	0.32	0.26	5
$5p^3P_1$–$5s^3S_1$	641.94	1	0.31	0.24	0.11	
$5p^3P_0$–$5s^3S_1$	645.82	3.5	0.48	0.3	0.05	
$5p^1P_1$–$5s^1S_0$	719.87	2	0.28		0.08	4
$5p^3P_2$–$6d^3D_3$	2061	40	4.1		1	
$5p^3P_1$–$4d^3D_2$	2139	20	4.1		0.5	
$5p^3P_1$–$4d^3D_1$	2128	20	5.5		0.25	
$5p^3P_0$–$4d^3D_1$	2169	20	5.5		0.27	
$5p^1P_1$–$4d^1D_2$	779.97	11	2.05		0.24	3.5*

* Optimal current density was not achieved.

Among the charge-transfer transitions in thallium and gallium of the same type, the lowest optimal current is observed for the transitions, where de-excitation by transitions (mostly by the *P*–*D* channel) is the least significant, and the cross section of partial charge transfer is smaller ($7p^3P_{1,0}$ of Tl II). Nevertheless, even for the $7p^3P_2^\circ$–$7s^3S_1$ transition in Tl II, it is just the de-excitation by electrons that is responsible for saturation of the output power.

The calculated results explain qualitatively the experimental time behavior of the laser power at lasing lines. Thus, for the 594.9-nm Tl II line, similarly to the situation described in Ref. 9 for the 615-nm Hg II line, as the current pulse of the optimum amplitude becomes longer, the gain and the output power saturate within 1.5–2 μs and then decrease, and at $\tau \geq 2.5$ μs the inversion breaks.

The calculations have shown that slow electrons do not change the level density of lasing $7p^3P_2^\circ$–$7s^3S_1$ Tl II levels at the discharge current density $J \leq 0.5$ A · cm^{-2} and the current pulse duration $\tau \leq 1$ μs. However, at longer pulses (about 1.5 μs and longer) the population inversion at the levels decreases sharply down to complete disappearance at $\tau \geq 3$ μs. This occurs mostly due to the de-excitation collisions of metal ions

with thermal electrons that decrease the level density of the upper lasing level and increase the density of neighboring 6^3D levels. The process of quenching is more significant for Tl II transitions from the levels $7p^3P_{1,0}$ energetically close to the levels 6^3D. It should be emphasized that in the HCD laser this process becomes possible, due to the specific electron energy distribution, not only in the afterglow of the discharge plasma (as in positive column), but also during the current pulse.

It is obvious that as the current pulse becomes longer, the optimum amplitude of the current must decrease for n_e does not exceed n_e^{critical}. It is just this effect that is observed experimentally. It qualitatively demonstrates the significance of taking into account the electron de-excitation for all transitions. On the contrary, in the first fractions of a microsecond, because of small n_e, the process of electron de-excitation becomes to play the role at a several times higher current. In this case, the rate of transition excitation by fast electrons for such τ, when $n_e < n_e^{\text{critical}}$, is by the same factor higher.

It is seen from Tables 2a and b that in addition to P–S transitions, lasing at which was observed earlier, this analysis points to the existence of inversion and, consequently, predicts the possibility of lasing at the IR transition of Hg II with $\lambda = 3016$ nm, four IR transitions of Tl II in the range of 1385–3179 nm, most intense of which have $\lambda = 1922$ and 1385 nm, and three transitions of Ga II in the range of 2061–2169 nm, the most intense of which has $\lambda = 2061$ nm. The unsaturated gain at these IR transitions exceeds by four to six times the gain at the most intense $7p^3P_2$–$7s^3S_1$ transition of Tl II and $5p^3P_2$–$5s^3S_1$ transition of Ga II, and the value of n_e^{critical} is an order of magnitude higher, what extends the range of the amplitude and duration of a current pulse needed in the experiment.

Acknowledgments

This work was supported in part by the Russian Foundation for Basic Research (Grant No. 99–02–17539) and the Ministry of Education of the RF (Grant No. E20–3.2–157).

References

1. I.G. Ivanov, E.L. Latush, and M.F. Sem, *Ion Metal Vapor Lasers* (Energoatomizdat, Moscow, 1990), 256 pp.
2. I.G. Ivanov, E.L. Latush, and M.F. Sem, *Metal Vapour Ion Lasers: Kinetic Processes and Gas Discharges* (Wiley, Chichester–New York–Brisbane–Toronto–Singapore, 1996), 285 pp.
3. S.P. Zinchenko, I.G. Ivanov, and M.F. Sem, Proc. SPIE **2110**, 150–165 (1993).
4. I.G. Ivanov and M.F. Sem, Electronics. Ser. 4. Electrovacuum and Gas-Discharge Devices, No. 4, 12–16 (1974).
5. V.V. Vainer, S.P. Zinchenko, I.G. Ivanov, and M.F. Sem, Zh. Prikl. Spektrosk. **31**, No. 5, 905–907 (1979).
6. M.G. Grozeva, N.V. Sabotinov, and M. Janossy, Opt. Quantum Electron. **18**, No. 2, 455–459 (1986).
7. S.P. Zinchenko, I.G. Ivanov, and M.F. Sem, in: *Abstracts of Reports at the Meeting on Population Inversion and Lasing at Atomic and Molecular Transitions* (Tomsk, 1986), Part. 1, p. 146.
8. I.G. Ivanov and A.Yu. Pimonov, J. Moscow Phys. Soc. **7**, No. 4, 371–377 (1997).
9. S.P. Zinchenko, I.G. Ivanov, E.L. Latush, and M.F. Sem, Opt. Spektrosk. **58**, No. 2, 302–306 (1985).
10. Landolt–Börnstein, Atom und Molecular Physik, Teil 5, Bd 1. (1950), 560 pp.
11. L.M. Biberman, V.S. Vorob'ev, and I.T. Yakubov, *Kinetics of Inequilibrium Low-Temperature Plasma* (Nauka, Moscow, 1982), 375 pp.
12. V.V. Vainer, G.A. Kalinchenko, and I.G. Ivanov, Fizika Plazmy **16**, No. 4, 460–466 (1990).
13. V.I. Bylkin, Opt. Spektrosk. **29**, No. 6, 1036–1042 (1970).
14. I.G. Ivanov and M.F. Sem, Electronics. Ser. 4. Electrovacuum and Gas-Discharge Devices, No. 10, 42–46 (1974).
15. H. Kano, T. Shay, and G.J. Collins, Appl. Phys. Lett. **27**, No. 11, 610–612 (1975).
16. E.L. Latush, M.F. Sem, and G.D. Chebotarev, Izv. Vyssh. Uchebn. Zaved. SSSR, Ser. Fiz., No. 5, 90–97 (1984).
17. O.P. Bochkova, I.A. Ivakin, V.N. Ostrovskii, Yu.A. Tolmachev, and A.V. Kuligin, Opt. Spektrosk. **67**, No. 3, 510–516 (1989).
18. A.K. Belyaev and J. Grosser, J. Phys. B: At. Mol. Opt. Phys. **29**, 5843–5855 (1996).
19. A.R. Turner-Smith, J.M. Green, and C.E. Webb, J. Phys. B: At. Mol. Phys. **6**, No. 1, 114–130 (1973).
20. E.N. Pavlovskaya and N.V. Podmoshenskii, Opt. Spektrosk. **34**, No. 1, 19–23 (1973).
21. A.I. Ogoyski et al., J. Phys. B: At. Mol. Phys. **32**, No. 9, 5479–5488 (1999).